ELSEVIER

Chemical Engineering Journal 114 (2005) 1–7

Chemical Engineering Journal

www.elsevier.com/locate/cej

Liquid mixing and gas–liquid mass transfer in a three-phase inverse turbulent bed reactor

Omar Sánchez [a,*], Sébastien Michaud [b], Renaud Escudié [b], Jean-Philippe Delgenès [b], Nicolas Bernet [b]

[a] *Departamento de Ingeniería Química, Universidad Católica del Norte, Avenida Angamos 0610, Antofagasta, Chile*

[b] *Laboratoire de Biotechnologie de l'Environnement (LBE), Institut National de la Recherche Agronomique (INRA), Avenue des étangs, 11100 Narbonne, France*

Received 19 October 2004; received in revised form 4 July 2005; accepted 24 August 2005

Abstract

In this research work, hydrodynamic characteristics and gas–liquid mass transfer in a laboratory scale inverse turbulent bed reactor were studied. In order to characterize internal flow in the reactor, the residence time distribution (RTD) was obtained by the stimulus-response technique using potassium chloride as a tracer. Different solid hold-up (0–0.37) and air superficial velocity (2.7–6.5 mm s^{-1}) values were assayed in RTD experiments. The parameters that characterize the RTD curve, mean residence time and variance were independent of the solid hold-up, thus the solid particle concentration did not influence liquid mixing in the reactor. The hydrodynamic of the inverse turbulent bed was well represented by a model that considers the reactor as two-mixed tank of different volumes in series. The value of the volumetric gas–liquid mass transfer coefficient ($k_L a$) was independent of the solid hold-up. This result enhances a previously suggested hypothesis, which considers that the solid and liquid form a pseudo-fluid in the inverse turbulent bed reactor.

Keywords: Fluidization; Mass transfer; Mixing; Moving bed; Multiphase reactors; Modeling

1. Introduction

Biofilm reactors with microorganisms naturally attached on small suspended particles, e.g. fluidized bed, airlift reactor, inverse fluidized bed and circulating bed reactor [1–5] have been used for organic matter and ammonia removal from domestic and industrial wastewaters. Compared to the activated sludge system, higher biomass concentration can be obtained in biofilm reactor, and higher volumetric loading rate of pollutants can be treated at the required removal efficiency. When microorganisms required for biological transformation of certain pollutants in a wastewater have low growth rates and yields, such as the nitrifying microorganisms (ammonia-oxidizing bacteria, $\mu_{max} = 0.014–0.092\ h^{-1}$ and nitrite-oxidizing bacteria, $\mu_{max} = 0.006–0.06\ h^{-1}$) or the methanogenic (aceticlastic methanogens, $\mu_{max} = 0.003–0.014\ h^{-1}$) [6], the use of biofilm reactors offers several advantages for treatment of this type of wastewater [7].

The inverse turbulent bed (ITB) is a three-phase reactor recently applied for anaerobic treatment of winery wastewater [8]. In this reactor, bed expansion was induced by injection of biogas (CH_4 and CO_2) at the bottom of the reactor. The ITB can also be used for aerobic wastewater treatment by injecting air instead of biogas. As a result, nitrification or aerobic matter removal can be carried out in this reactor [9].

Liquid recycling is not necessary to induce bed expansion in the ITB, and this is an advantage compared to the operation of two-phase fluidized bed and two-phase inverse fluidized bed reactors. Superficial air velocity in ITB is lower than in other biofilm reactors, i.e. airlift and three-phase fluidized bed reactors, since particles of low density and small diameter are used as support. This decreases the energy cost for support expansion.

Hydrodynamic studies in ITB have been carried out in reactor filled with particles of different densities ranging from 106 to 934 kg m^{-3} [10–12]. These works focused mainly on establishing bed expansion characteristics at different gas and liquid superficial velocities. However, hydrodynamic studies aiming liquid mixing model determination in ITB reactors have received less attention. Although, flow models are scale dependent, availability of hydrodynamic model for laboratory scale reactors may

* Corresponding author. Tel.: +56 55 355904; fax: +56 55 355917.
E-mail address: osanchez@ucn.cl (O. Sánchez).

1385-8947/$ – see front matter © 2005 Elsevier B.V. All rights reserved.
doi:10.1016/j.cej.2005.08.009

Nomenclature

A	cross-sectional area of the column (m^2)
C_i	tracer concentration ($mg\,l^{-1}$)
C_o	oxygen concentration in the liquid ($mg\,l^{-1}$)
C_o^*	saturation oxygen concentration ($mg\,l^{-1}$)
C_p	oxygen concentration probe response ($mg\,l^{-1}$)
d_p	mean support diameter (mm)
D	distance between particles (mm)
E,E'	dimensionless residence time distribution function
H	bed height (m)
k_La	volumetric air liquid mass transfer coefficient (s^{-1})
M	mass of solid (kg)
Pe	Peclet number dimensionless
t_i	time (s)
U_g	superficial air velocity ($m\,s^{-1}$)
U_l	superficial liquid velocity ($m\,s^{-1}$)
V_{R1}	volume of the first reactor (l)
V_{R2}	volume of the second reactor (l)

Greek letters

ε_s	solid hold-up of the bed
ε_{s0}	solid hold-up of the fixed bed
ρ	solid density ($kg\,m^{-3}$)
μ_{max}	maximum specific growth rate (h^{-1})
τ	probe constant (s^{-1})
θ,θ'	dimensionless time

improved model predictions from studies carried out in this type of reactors.

Mass transfer characteristics of ITB reactor have received less attention than its hydrodynamic behavior. In other three-phase reactors, the air–liquid mass transfer rate has been measured [13–15], but results about the influence of solid hold-up on the gas–liquid mass transfer coefficient are not conclusive.

The objectives of this work were to investigate the flow pattern and the gas–liquid mass transfer capacity of a laboratory-scale ITB reactor. Residence time distribution and volumetric gas–liquid mass transfer coefficient in the reactor was measured at different solid hold-up and superficial air velocity. Based on the obtained data, a flow model for the ITB is proposed, relevant mixing characteristics of this reactor are discussed and gas–liquid mass transfer characteristics are compared with other biofilm reactors.

2. Materials and methods

The schematic diagram of the experimental set-up is shown in Fig. 1. The reactor consisted of a PVC column of 0.054 m internal diameter. The height of the fluidization section between the air injection point and the liquid level was 0.55 m. The solid support was extendosphere (PQ Hollows Spheres Ltd) of 0.150 mm in diameter and 690 $kg\,m^{-3}$ in density. The main component of this solid material is SiO_2 (55–60%). The fixed bed solid hold-up ε_{s0} was 0.62.

Flow model determination was carried out using data obtained from stimulus-response experiments [16]. The tracer used was a solution of KCl, 3 M. In each experiment, 1 ml of this solution was injected into the water stream entering the reactor at a flow rate of 1.5 L h^{-1}. Conductivity values were continuously

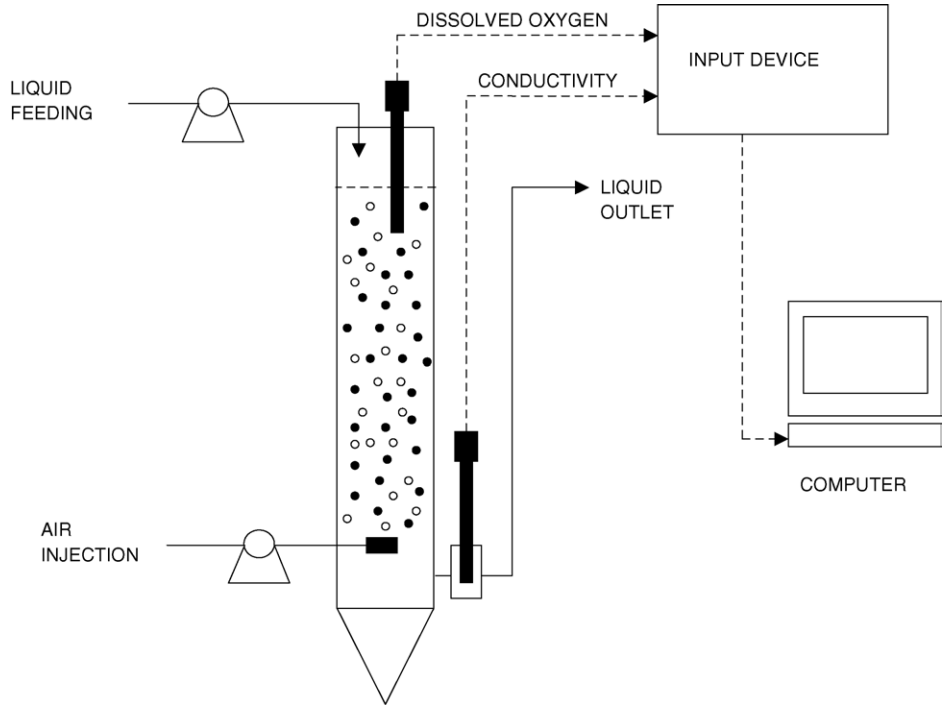

Fig. 1. Inverse turbulent bed reactor with conductivity and dissolved oxygen on-line measuring device.

measured in the effluent using a conductivity sensor (WTW LF 325, Germany) coupled to a data acquisition card connected to a PC. The duration of the experiment was four times longer than the average detention time (t_a). Different values of solid hold-up (0–0.37) were tested at a constant superficial air velocity, $U_g = 5.64\,mm\,s^{-1}$. The effect of superficial air velocity on liquid mixing was assessed in the range between 2.7 and 6.5 mm s^{-1}, for constant solid hold-up of 0.185. Under these operating conditions, the gas hold-up (ε_g) values ranged between 0.02 and 0.04. The solid hold-up was calculated as

$$\varepsilon_s = \frac{M}{AH\rho} \tag{1}$$

where M is the mass of solid (kg), A the cross-sectional area of the column (m^2), H the bed height (m), and ρ is the solid density (kg m^{-3}).

The average detention time in the fluidized bed was calculated as follows:

$$t_a = \frac{V\varepsilon_l}{Q} \tag{2}$$

where V is the volume of the fluidized bed, ε_l the liquid hold-up, and Q is the volumetric flow rate through the reactor.

From each residence time distribution (RTD) curve obtained, experimental mean residence time (t_e) and variance (σ_t^2) were calculated:

$$t_e = \frac{\sum t_i C_i \Delta t_i}{\sum C_i \Delta t_i} \tag{3}$$

$$\sigma_t^2 \frac{\sum t_i^2 C_i \Delta t_i}{\sum C_i \Delta t_i} - t_e^2 \tag{4}$$

The air–liquid mass transfer coefficient was estimated at different values of the solid fraction, superficial air velocity and superficial liquid superficial velocity. Solid hold-up was varied between 0.03 and 0.19, superficial air velocity between 0.6 and 9 mm s^{-1} and superficial liquid velocity between 0.1 and 0.95 mm s^{-1}. In all experiments, the volumetric oxygen transfer coefficient was estimated from the dynamic response of dissolved oxygen concentration after nitrogen injection was switched to air injection. Zero oxygen concentration was always ensured before air injection began. The increase in dissolved oxygen concentration in the liquid was measured using an oxygen probe (Mettler Toledo, O_2 4100, Switzerland), and the data were recorded on a computer equipped with a data acquisition card.

Eq. (5) represents the dissolved oxygen mass balance in the liquid phase of the ITB reactor. The dynamic response of the system, observed in the dissolved oxygen probe, can be simplified as a delay [15,17] and it was represented using a first-order model (Eq. (6)). Eqs. (5) and (6) form a system of two coupled ordinary differential equations that must be solved simultaneously:

$$\frac{dC_o}{dt} = k_L a(C_o^* - C_o) \tag{5}$$

$$\frac{dC_p}{dt} = \frac{1}{\tau}(C_o - C_p) \tag{6}$$

where C_o is the oxygen concentration in the liquid (mg l^{-1}), $k_L a$ the volumetric air liquid mass transfer coefficient (s^{-1}), C_o^* the saturation oxygen concentration ($T = 30\,^\circ C$, $C_o^* = 7.5$ mg l^{-1}), C_p the oxygen concentration probe response (mg l^{-1}), and τ is the probe constant (s^{-1}).

The delay time of the probe was experimentally measured (52 s) and agreed with the value reported by the manufacturer's probe. The initial conditions for solving simultaneously Eqs. (5) and (6) are

$$t = 0, \qquad C_o = 0, \qquad C_p = 0 \tag{7}$$

Estimation of the gas–liquid mass transfer coefficient was based on minimization of the difference between the liquid oxygen concentrations measured experimentally and the value predicted by solving Eqs. (5) and (6). Calculations were made using a code that combines the Runge–Kutta method and a minimization routine.

3. Results and discussion

3.1. Mixing experiments

In these experiments, the effect of the solid fraction and the superficial gas velocity on mixing in the ITB was investigated. In Fig. 2, RTD curves for three different values of the solid fraction ($\varepsilon_s = 0$, 0.25 and 0.37) are presented in dimensionless form ($E(\theta)$):

$$\text{where } \theta = t/t_a \tag{8}$$

$$\text{and } E(\theta) = \frac{C(\theta)}{(Q/V)\sum C_i \Delta t_i} = \frac{C(\theta)}{\left(\sum C_i \Delta t_i\right) t_a} \tag{9}$$

Experimental mean residence time (t_e) and variance (σ_t^2) allow to characterize the RTD curve and by comparing their values, it is therefore possible to evaluate the effect of the solid fraction on mixing in the ITB. For all the solid fractions assayed, Fig. 3 presents these two parameters in dimensionless form: t_e/t_a

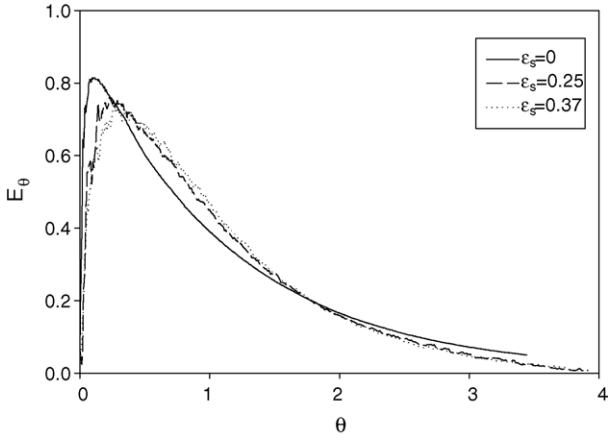

Fig. 2. Residence time distribution ($E(\theta)$) for the inverse turbulent bed reactor at different solids hold-up.

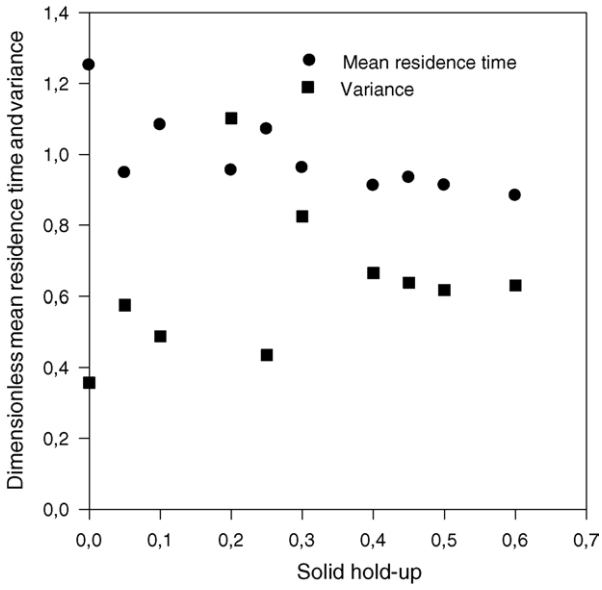

Fig. 3. Dimensionless mean and variance of the RTD curves as a function of solid hold-up.

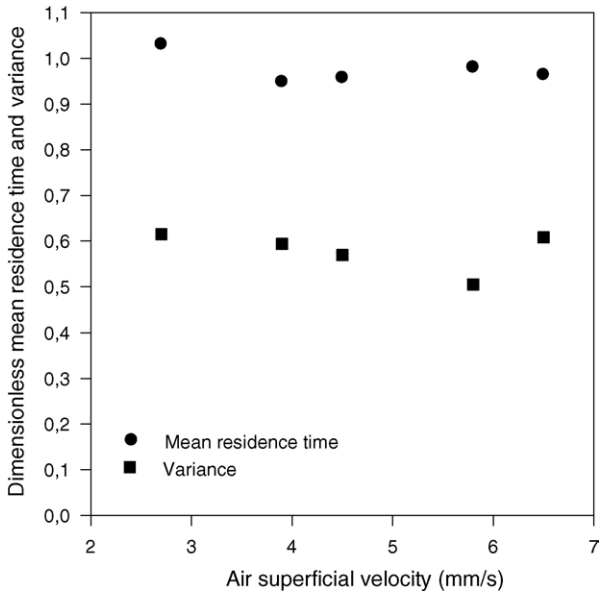

Fig. 4. Dimensionless mean and variance of the RTD curves as a function of superficial air velocity.

and $\sigma_\theta^2 = \sigma_t^2/t_a^2$. For solid hold-up values greater than 0.3, the mean residence time was lower than 1, and the variance was greater than 0.6. Apparently these results indicate that when the solid hold-up increased over 0.3, mixing in the ITB was affected by the solid hold-up. In order to assess the effect of solid hold-up on reactor mixing, two groups were formed with mean residence time and variance data: values obtained at solid hold-up lower than 0.3 formed one group and values obtained at solid hold-up greater than 0.3 formed the other. A *F*-test was carried out at the 95% confidence level and not statistically significant difference ($p > 0.5$) between the two groups was found, when the mean residence time and the variance data were compared. Thus, solid hold-up did not affect the mixing in the ITB, under the operating conditions of this work. Consequently, the dead region caused by the solid support is not detected and the whole liquid volume is mixed.

The results herein reported disagree with those obtained by Comte et al. [10] who observed a better mixing in the presence of support. This could be explained by the difference in size and density of the solid particles used as support. In our case, the density and diameter of the particles are lower than those used by Comte et al. [10]. Thus, they cannot break the bubble roofs and are expanded by the circulating effect mostly due to the motions induced by the bubble rise in the reactor [11]. The solid particles are much smaller than the bubbles. Here, the pseudo-fluid is not constituted by the mixed gas and liquid phases like in the work of Comte et al. [10], but by the solid and liquid phases.

The experimental mean residence time (t_e) and variance (σ_t^2) at a constant solid fraction ($\varepsilon_s = 0.185$) and at different gas superficial velocity are presented in Fig. 4. When the superficial gas velocity was varied between 2.7 and 6.5 mm s^{-1}, the mixing efficiency in the ITB was not affected, as indicated by the constant values of t_e/t_a (1) and of σ^2/t_a^2 (0.6).

In a previous study about mixing in the ITB reactor, the value of the Peclet number, *Pe*, was calculated from the RTD curves [18]. Since the value of *Pe* ranged between 1.78 and 2.37, a model of two continuous stirred tank reactors in series ($CSTR_\alpha$) of different volumes was used to represents mixing in the ITB reactor [19]:

$$E'(\theta') = \frac{\exp\left(-\frac{\theta'}{a} - \exp\right)\left(-\frac{\theta'}{1-a}\right)}{2a-1} \tag{10}$$

$$\text{with } a = \frac{V_{R2}}{V_{R1} + V_{R2}} \tag{11}$$

where V_{R1} is the volume of the first reactor and V_{R2} is the volume of the second reactor.

The only parameter of this model is α, that represents the ratio between the volumes of the two theoretical reactors. In Fig. 5, for a solid fraction of 0.283 and superficial gas velocity 5.64 mm s^{-1}, the experimental $E(\theta)$ curve is compared with three model predictions: one completely mixed reactor (CSTR), two

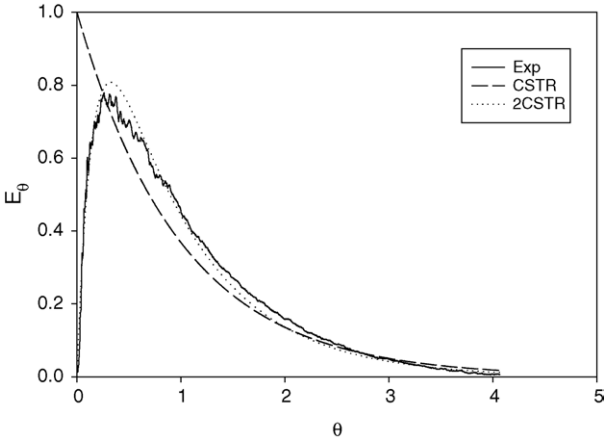

Fig. 5. Comparison of experimental RTD data with model prediction; one mixed reactor model (CSTR) and two mixed reactor model (2CSTR).

Table 1
Value of alpha in the model of two continuous stirred tank reactors

U_g (mm s^{-1})	ε_s	Alpha	V_{R1}/V_{R2}	ε_s	U_g (mm s^{-1})	Alpha	V_{R1}/V_{R2}
5.64	0	0.956	21.5	0.189			
	0.047	0.949	18.6		2.71	0.853	5.8
	0.094	0.916	10.9		3.95	0.835	5.1
	0.189	0.854	5.9		4.52	0.855	5.9
	0.236	0.817	4.4		5.87	0.852	5.7
	0.283	0.814	4.4		6.55	0.858	6.0
	0.377	0.804	4.1		6.55	0.861	6.2
	0.425	0.817	4.5		6.55	0.871	6.7
	0.472	0.798	4.0				
	0.566	0.806	4.2				

completely mixed reactors of similar volume in series ($CSTR_2$) and $CSTR_\alpha$.

The model of two completely mixed reactors in series with $\alpha = 0.817$ shows a better agreement with the experimental data than the two other models. Two continuous stirred tank reactor model (equivalent to a $CSTR_\alpha$ with $\alpha = 0.5$) are not able to predict the location of the maximal value of the experimental RTD curve. By using curve fitting, the value of α was calculated from all the experimental data set (Table 1).

When the reactor corresponds to a bubble column ($\varepsilon_s = 0$), α is equal to 0.956 and the ratio between the volume of the first theoretical reactor and the second one is 20. For solid hold-up value lower than 0.25 ($U_g = 5.64$ mm s^{-1}), α value decreases and reaches 0.817 at $\varepsilon_s = 0.236$: in this operating condition, the ratio V_{R1}/V_{R2} corresponds to 4.4. Starting from a solid hold-up of 0.283, the parameter of $CSTR_\alpha$ is quite constant (4–4.5). It is not surprising to observe that the gas superficial velocity did not influence α because experimental mean residence time (t_e) and variance (σ_t^2) were shown to be constant.

Concerning the influence of the particle diameter and the gas superficial velocity on the mixing characteristics of three-phase reactors, it has been reported that in fluidized bed reactor when the diameter of the particle used decreases from 6 to 0.25 mm [20], and in inverse fluidized bed when gas superficial velocity increases between 0 and 0.7 mm s^{-1} [21], the axial dispersion coefficient increases, and so mixing also increases. Comparing our results and experimental operation conditions with those occurring in the formerly cited works, it seems that the use of particles of small diameter and high gas superficial velocity induces a high degree of mixing in the ITB.

3.2. Gas–liquid mass transfer experiments

Fig. 6 shows gas–liquid mass transfer coefficient (k_La) values in the laboratory ITB reactor at different solid hold-up. An increase of k_La values was observed as the air velocity was increased, both in the reactor filled with particles and in the reactor without particles. However, k_La values in reactor without particles was greater than in reactor filled with particles at all solid hold-up tested. As the solid hold-up increased, the difference between the k_La values in the reactor charged with particles and the reactor not filled with particles increased.

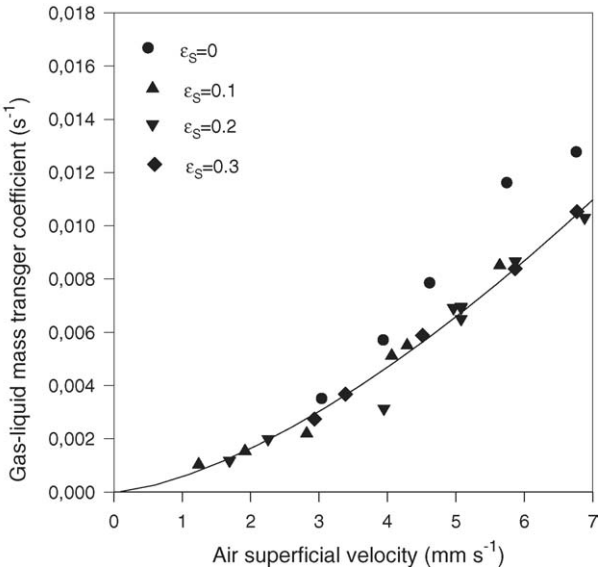

Fig. 6. Gas–liquid mass transfer coefficient in the inverse turbulent bed reactor. Symbols indicate different solid hold-up and line indicates fitted correlation using only data from reactor charged with particles.

The following equation fitted the k_La values as a function of the air velocity U_g. Data from the experiments in the ITB reactor without particles were not used to obtain this equation:

$$k_La = 5.7 \times 10^{-4}\, U_g^{1.52} \tag{12}$$

The experimental data and the prediction of the correlation are presented in Fig. 6. The mathematical form of the correlation is in accordance with results obtained in a two-phase reactor without support [14]. This suggests that this solid-water system behaves like a liquid, with respect to its gas–liquid mass transfer properties, enhancing the model of a solid–liquid pseudo-fluid. This phenomenon has been also observed in others three-phase systems [22]. In fact, gas–liquid mass transfer in slurry reactors have been modeled using models developed for gas–liquid systems assuming that the solid–liquid phase can be treated as a pseudo-liquid phase [22]. The low diameter of the particles used in slurry reactor could explain this behavior. As ITB reactor also uses particles of low diameter, theoretically, the extendosphere particles–water system could be treated as a liquid system. This assumption is in agreement with the experimental results obtained in this work. In a three-phase system, k_La can also depend on particles density [23]. However, as the density of the extendosphere particles is low, gas bubbles are not easily broken by the solid particles.

Many studies concerning the gas–liquid mass transfer in inverse fluidized-bed reactors have not considered the effect of solid concentration [13,24]. In three-phase up-flow fluidized bed reactors, the effect of the solid hold-up has received attention [2,14,15,25]. With particles without biofilm, it was reported that k_La values increased with the solid fraction in reactor filled with sand particles [2] but as the solid fraction increase in reactor filled with basalt particles k_La decrease [15]. The diameter and density of both, sand and basalt, particles used in these studies are higher than that of the extendosphere particles used in this work.

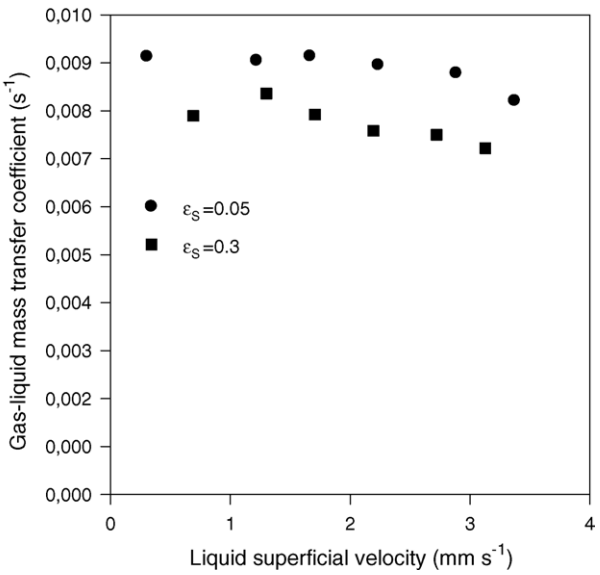

Fig. 7. Gas–liquid mass transfer coefficient in the inverse turbulent bed reactor at different superficial liquid velocities. Symbols indicate different solid hold-up.

This comparison suggests that the effect of solid concentration on k_La depends on particles characteristics. In a three-phase internal loop airlift gas–liquid mass transfer was studied in a reactor filled with 175 μm silica sand [26]. It was reported that k_La dependence on solid hold-up was moderated. The diameter of these sand particles is very similar to the extendosphere particles used in the ITB reactor.

In biofilm suspension reactor, the biofilm growth causes a decrease in the overall particle density value since the biomass density is lower than the particles density. According to the results of the present work, as bioparticle density approaches water density value, the influence of solid concentration on k_La values could be negligible since the system could behave like a two-phase reactor. Ryhiner et al. [2] found that the k_La value was independent of the solid fraction in three-phase biofilm reactors, but Nicolella et al. [15] reported that when solid fraction was increased the k_La value decreased. Nevertheless, comparing the results of Nicolella et al. [15] in reactor filled with clean particles and with particles with biofilm, only a slow decrease of the k_La value was noted when the gas velocity value increased in the former reactor. With particles of density values equal to 1180 and 1600 kg m^{-3}, k_La has been shown to be independent of the solid fraction in fluidized-bed reactors at ε_s values lower than 0.3 [2]. Further research on the relationship between the solid density and the particle coalescence would be helpful to explain these results. In a range of liquid velocities between 0.1 and 1 mm s^{-1}, at which the inverse turbulent bed reactor are generally operated [11], the k_La is independent of this parameter (Fig. 7).

4. Conclusions

The objectives of this work were to study the liquid mixing and the air–liquid oxygen transfer in an inverse turbulent bed reactor. As the parameters that characterize the residence time distribution were constant at varying solid hold-up, it can be concluded that the reactor behaves like a two-phase reactor, the liquid and solid phases behaving like a homogenous pseudo-fluid. Possible dead regions caused by the solid support were not detected. The hydrodynamics in the ITB was independent of the superficial air velocity. The ITB reactor flow pattern could be described by a two-mixed reactors of different sizes in series model. The air–liquid mass transfer rate was independent both of the solid hold-up and the superficial liquid velocity. This result is different from observations made using inverse turbulent bed reactor with a different carrier. Therefore, the ITB reactor behavior depends on the solid carrier characteristics, especially size and density.

References

[1] H. Tanaka, I.J. Dunn, Kinetics of biofilm nitrification, Biotechnol. Bioeng. 24 (1982) 669–689.
[2] G. Ryhiner, S. Petrozzi, I.J. Dunn, Operation of a three-phase biofilm fluidized sand bed reactor for aerobic wastewater treatment, Biotechnol. Bioeng. 32 (1988) 677–688.
[3] L. Tijhuis, J.L. Huisman, H.D. Hekkelman, M.C.M. van Loosdrecht, J.J. Heijnen, Formation of nitrifying biofilms on small suspended particles in airlift reactors, Biotechnol. Bioeng. 47 (1995) 585–595.
[4] D.G. Karamanev, L.N. Nikolov, Application of inverse fluidization in wastewater treatment: from laboratory to full scale bioreactors, Environ. Prog. 15 (3) (1996) 194–196.
[5] V. Lazarova, R. Nogueira, J. Manem, L. Melo, Control of nitrification efficiency in a new biofilm reactor, Water Sci. Technol. 36 (1) (1997) 31–41.
[6] C.P.L. Grady Jr., G.T. Daigger, H.C. Lim, Biological Wastewater Treatment, 2nd ed., Marcel Dekker, New York, 1999.
[7] C. Nicolella, M.C.M. van Loosdrecht, J.J. Heijnen, Particle-based biofilm reactor technology, TIBTECH 18 (2000) 312–320.
[8] P. Buffière, J.P. Bergeon, R. Moletta, The inverse turbulent bed: a novel bioreactor for anaerobic treatment, Water Res. 34 (2) (2000) 673–677.
[9] N. Bernet, O. Sanchez, P. Dabert, A. Olaïzola, J.J. Godon, J.P. Delgenès, Effect of solid hold-up on nitrite accumulation in a biofilm reactor—molecular characterization of nitrifying communities, Water Sci. Technol. 49 (11/12) (2004) 123–130.
[10] M.P. Comte, D. Bastoul, G. Hébrard, M. Roustan, V. Lazarova, Hydrodynamics of a three-phase fluidized bed the inverse turbulent bed, Chem. Eng. Sci. 52 (1997) 3971–3977.
[11] P. Buffière, R. Moletta, Some hydrodynamic characteristics of inverse three phase fluidized-bed reactors, Chem. Eng. Sci. 54 (1999) 1233–1242.
[12] P. Legile, G. Menard, C. Laurent, D. Thomas, A. Bernis, Contribution a l'étude hydrodynamique d'un lit fluidisé triphasique inverse fonctionnant à contre-courant, Entropie 143/144 (1988) 23–31.
[13] C. Shimodaira, Y. Yushina, Biological waste water treatment with downflow fluidized bed reactor, in: Proceeding of the Third Pacific Congress of Chemical Engineering, 1983, pp. 237–242.
[14] K. Nguyen-Tien, A.N. Patwari, A. Shumpe, W. Deckwer, Gas–liquid mass transfer in fluidized particle beds, AIChE J. 31 (2) (1985) 194–201.
[15] C. Nicolella, M.C.M. van Loosdrecht, R.G.J.M. van der Lans, J.J. Heijnen, Hydrodynamic characteristics and gas–liquid mass transfer in a biofilm airlift suspension reactor, Biotechnol. Bioeng. 60 (1998) 627–635.
[16] O. Levenspiel, Chemical Reaction Engineering, 2nd ed., John Wiley & Sons, New York, 1972.
[17] T. Philichi, M. Stenstrom, Effects of dissolved oxygen probe lag on oxygen transfer parameter estimation, J. Water Pollut. Contr. Fed. 61 (1) (1989) 83–86.

[18] S. Michaud, Etude hydrodynamique et biologique dun procede de methanisation a biofilm: le reacteur a lit turbule inverse. Thèse de Doctorat, Université Montpellier II, France, 2001.
[19] J. Villermaux, Génie de la reaction chimique, 2éme ed., Lavoisier Tec and Doc, 1992.
[20] S.D. Kim, H.S. Kim, J.H. Han, Axial dispersion characteristics in three-phase fluidized beds, Chem. Eng. Sci. 47 (1992) 3419–3426.
[21] D. Garcia-Calderon, Hydrodynamique et conversion d'un réacteur anaérobie en fluidisation inverse. Thèse de Doctorat, Université Montpellier II, France, 1997.
[22] B. Zhao, J. Wang, W. Yang, Y. Jin, Gas–liquid mass transfer in a slurry–bubble system. I. Mathematical modeling based on a single bubble mechanism, Chem. Eng. J. 96 (2003) 23–27.
[23] W. Jianping, N. Ping, H. Lin, C. Yunlin, Local overall gas–liquid mass transfer coefficient in a gas–liquid–solid reversed flow jet loop reactor, Chem. Eng. J. 88 (2002) 209–213.
[24] J.Y. Hihn, P. Boldo, Y. Gonthier, A. Bernis, Tranfert d'oxygène dans un lit fluidisé triphasique inverse à contre-courant de gaz et de liquide, Methodologie-Résultats, Récents Progrès en Génie des Procédés 5 (16) (1991) 153–158.
[25] V. Bigot, B. Bataille, B. Capdeville, M. Roustan, J.M. Audic, Etude du tranfert d'oxygène dans les lits fluidisés triphasiques: influence de la présence de solide, Récents Progrés en Génie des Procédés 4 (10) (1990) 319–325.
[26] G. Olivieri, A. Marzocchella, P. Salatino, Hydrodynamyic and mass transfer in a lab-scale three-phase internal loop airlift, Chem. Eng. J. 96 (2003) 45–54.